Journal of Power Sources 189 (2009) 1231–1239

Contents lists available at ScienceDirect

Journal of Power Sources

journal homepage: www.elsevier.com/locate/jpowsour

Numerical modelling of a bromide-polysulphide redox flow battery. Part 2: Evaluation of a utility-scale system

Daniel P. Scamman [a], Gavin W. Reade [b,1], Edward P.L. Roberts [a,*,2]

[a] School of Chemical Engineering and Analytical Science, University of Manchester, Sackville St, P.O. Box 88, Manchester M60 1QD, UK
[b] Regenesys Technologies Limited, OTEF, Aberthaw Power Station, Barry, Vale of Glamorgan CF62 4QT, UK

ARTICLE INFO

Article history:
Received 2 December 2008
Received in revised form 22 January 2009
Accepted 25 January 2009
Available online 6 February 2009

Keywords:
Redox flow battery
Polysulphide bromide
Load-levelling
Arbitrage
Economic modelling

ABSTRACT

Numerical modelling of redox flow battery (RFB) systems allows the technical and commercial performance of different designs to be predicted without costly lab, pilot and full-scale testing. A numerical model of a redox flow battery was used in conjunction with a simple cost model incorporating capital and operating costs to predict the technical and commercial performance of a 120 MWh/15 MW utility-scale polysulphide-bromine (PSB) storage plant for arbitrage applications. Based on 2006 prices, the system was predicted to make a net loss of 0.45 p kWh^{-1} at an optimum current density of 500 A m^{-2} and an energy efficiency of 64%. The system was predicted to become economic for arbitrage (assuming no further costs were incurred) if the rate constants of both electrolytes could be increased to 10^{-5} m s^{-1}, for example by using a suitable (low cost) electrocatalyst. The economic viability was found to be strongly sensitive to the costs of the electrochemical cells and the electrical energy price differential.

1. Introduction

The demand for utility-scale energy storage is growing due to an increasing need for load-levelling. This need is driven by the power quality requirements for the digital economy, the decommissioning of old power plant and management of the output from renewable energy technologies (in particular wind power). The annual lost productivity in the US due to electricity outages and disruptions of all types was estimated to be about $119 billion in 2001 [1]. It has been estimated that there is a potential market for electricity storage of at least 10–15 GW p.a. based on the displacement of new capacity alone [2]. Redox flow batteries (RFBs) have been investigated for many years as chemical stores of electrical energy [3,4]. Theses systems are considered to be suitable for utility-scale energy storage, ideal for long-term load-shifting and for combinations of functions including spinning reserve, regulation control and power quality [1]. Redox couples currently under development for use in RFBs include polysulphide-bromine (PSB) [5–8], vanadium–vanadium [9,10], vanadium–polyhalide [11], cerium–zinc [12–14] and lead–lead [4].

Numerical modelling of redox flow battery systems for energy storage applications allows the technical and commercial performance of different designs to be predicted without costly lab, pilot and full-scale testing. RFB systems modelled to date include iron–chromium [15] and zinc–ferricyanide [16]. The PSB couple has been considered here for utility-scale arbitrage applications, which has been thought capable of achieving sales of approximately 5 GW p.a. at prices of £500 kW^{-1} [2]. A model of the bromide half-couple found that several reaction mechanisms could account for observed behaviour [17] and a review of zinc–bromide models reported recommendations for improving cell design [18].

In this study, the model developed in part 1 [19] is used to provide data on the technical performance of a 15 MW, 120 MWh utility-scale PSB RFB system. This is combined with a simple economic model including the main capital and operating costs to optimise the design and evaluate its commercial viability. The aim of the modelling was to determine the sensitivity of the economic performance of the system to fundamental parameters such as the electrochemical rate constants.

2. Technical model and design parameters

There are a large number of operating conditions which in practice will require optimisation. Key parameters include current density, electrolyte flow rate, operating temperature [20] and the concentration of the active species. The performance can be significantly affected by design parameters such as the inter-electrode gap, electrode materials and the solvent (e.g. organic electrolytes for a larger potential window [21]). In this study the electrolyte system and cell design is based on the Regenesys PSB electrolyte with

* Corresponding author. Tel.: +44 161 306 8849; fax: +44 161 306 9321.
E-mail address: Edward.roberts@manchester.ac.uk (E.P.L. Roberts).
[1] Present address: Rolls Royce plc, P.O. Box 31, Derby DE24 8BJ, UK.
[2] ISE member.

0378-7753/$ – see front matter © 2009 Elsevier B.V. All rights reserved.
doi:10.1016/j.jpowsour.2009.01.076

Nomenclature

a	annual inflation rate (%)
A	electrode area (m^2 $cell^{-1}$)
A_c	cross-sectional area of the flow channel (m^2)
C	cost (£)
C_{cap}	capital cost (£)
D	diffusion coefficient (m^2 s^{-1})
d_e	hydraulic diameter (m)
d_g	electrode gap (m)
E	cell voltage (V)
E^0	standard potential (V)
F	Faraday's constant (96,485 C mol^{-1})
g	electrode membrane gap (m)
i	current density (A m^{-2})
k_s	kinetic rate constant (m s^{-1})
k_m	mass-transport coefficient (m s^{-1})
L	electrode height (m)
M	molecular weight (kg mol^{-1})
N	number of cells
P_{mx}	maximum power consumption (W)
[P]	concentration of species P (mol dm^{-3})
$[P]_T$	total elemental concentration of species P (mol dm^{-3})
Δp	pressure drop (Pa)
Q	energy (J)
r	annual discount rate (%)
t_P	transference coefficient for species P (molecules $cation^{-1}$)
t	time (s)
Δt	time step (s)
T	temperature (K)
v	electrolyte velocity (m s^{-1})
V	electrolyte volume (m^3)
ΔV	the change in electrolyte volume (m^3)
w	electrode width (m)
z	number of electrons transferred in a reaction
z_P	stoichiometric coefficients of species P

Greek symbols

α	constant in power-law relationship
κ	conductivity (S m^{-1})
ν	kinematic viscosity (m^2 s^{-1})
π	energy efficiency
ρ	density (kg m^{-3})
σ	state-of-charge
ψ	extent of reaction per pass (mol m^{-3} $pass^{-1}$)
ω	net present value factor

Subscripts

BOC	bottom-of-charge value
Br	value for the bromide electrolyte
ch	charge value
del	delivered value
dis	discharge value
H_2O	water value
m	module (200 cells)
p	pump value
S	value for the sulphide electrolyte
T	total

Dimensionless numbers

Re	Reynolds number (vd_e/ν)
Sc	Schmidt number (ν/D)
Sh	Sherwood number ($k_m d_e/D$)

multiple bipolar stacks [22]. The cell geometry, electrode materials, electrolyte composition and operating temperature were fixed on this basis. The study focuses on the optimisation of the current density and the sensitivity of the economic performance to the electrochemical system properties, in particular, the electrochemical kinetics.

The details of the numerical model of the electrochemical performance have been described in part 1 [19]. The design of the 'XL' electrochemical cell (used in the 'XL200' bipolar stack) has been discussed in detail elsewhere [22]. It consisted of 0.67 m^2 activated carbon electrodes pressed into polymer frames, a cation-selective membrane taken to have the properties of Nafion 117, a turbulence-promoting mesh and manifolds containing spiral channels to reduce shunt currents.

Electrolytes were circulated through the cell and stored in separate tanks, with the concentration of reactants and products in the tanks gradually decreasing and increasing respectively during half-cycles. Sodium ions migrated through the membrane to maintain electroneutrality (hydrogen ions were not the main charge-carrier due to their low concentration [23]). The properties of the electrolytes and membrane, along with other key parameters, are summarised in Table 1 [24]. The state-of-charge (σ) of each electrolyte is defined as

$$\sigma_{Br} = \frac{[Br_2]}{[Br_2] + (1/2)[Br^-]} \quad (1)$$

$$\sigma_S = \frac{[S^{2-}] - (1/4)[S]}{[S^{2-}] + [S]} \quad (2)$$

The model of the process [19] was calculated the variation with time of cell voltage, current distribution, species concentrations and electrolyte volume. A constant current was applied and the cell voltage variation was calculated over each half-cycle. The numerical errors in voltage, efficiency, power density and energy density were limited to 10^{-4}, provided suitable numerical parameters were used [24]. For the conditions studied, a time step Δt of 20 min was suitable and the electrode was divided into 30 segments in order to calculate the current distribution. This was sufficient provided the extent of reaction per pass ψ did not exceed 0.39 M $pass^{-1}$ for the bromide ions. The extent of reaction per pass can be calculated as

$$\psi = \frac{z_P}{z}\frac{iA}{F\nu A_c} \quad (3)$$

where z_P/z is the ratio of the stoichiometric coefficients of the reactant species and the electrons transferred, i is the current density, ν is the average electrolyte velocity, A is the electrode area and A_c is the flow cross-sectional area. The model included the effects of electro-osmosis of water and self-discharge due to sulphide diffusion across the membrane. Key assumptions were plug flow, constant voltage along the electrode, constant conditions across the width and depth of the module, and 100% current efficiency. In bipolar stacks shunt currents can cause a loss of current efficiency of up to 4% in some systems [25]. However, in this study the shunt currents are assumed to be negligible due to the use of spiral manifolds which increase the electrical resistance between each cell and the manifold.

2.1. Electrolyte volume variation due to cross-membrane water transport

The model included the electrolyte volume variation during half-cycles due to water transport across the membrane accompanying the sodium ions. The bromide system decreased in volume on charge while the sulphide system increased, and *vice versa*. A reference volume, the volume of each electrolyte encountered at bottom-of-charge, V_{BOC}, was used. It was assumed that equal vol-

Table 1
Bipolar stack (XL200) and PSB electrolyte properties [24].

System properties	Symbol	Value
Electrode area	$A\,(m^2)$	0.67
Electrode height	$L\,(m)$	1.08
Electrode width	$W\,(m)$	0.668
Hydraulic electrode diameter	$d_e\,(mm)$	1.9
Half-cell cross-sectional area	$A_c\,(m^2)$	6.35×10^{-4}
Cycle length	$T_{ch}\,(h)$	8
Number of cells	$N\,(cells)$	200 cells per module
Operating temperature	$T\,(K)$	308
Water transference coefficient	t_{H_2O}	10 moles of water per mole Na^+ ions transferred

Half-cell properties		Bromide	Sulphide
Standard redox potential	$E^0\,(V)$	+1.09	−0.48
Electrons transferred	Z	2	2
Kinetic rate constant	$k_s\,(\times 10^{-8}\,m\,s^{-1})$	40	3
Total elemental concentrations at V_{BOC}	$[P]_T\,(M)$	4.5	4.8
Minimum state-of-charge	σ_{BOC}	0.1	0.069
Maximum state-of-charge	σ_{TOC}	0.498	0.302
Mass-transport correlation	–	$Sh = 0.081Re^{0.89}Sc^{0.33}$	$Sh = 0.099Re^{0.69}Sc^{0.33}$
Mass transport correlation validity range		$20 < Re < 120$	$20 < Re < 150$
Pressure-drop relationship	–	$\frac{\Delta p}{\rho v^2} = 85,000\left(\frac{v d_e}{\nu}\right)^{-0.4} + 55,000$	$\frac{\Delta p}{\rho v^2} = 85,000\left(\frac{v d_e}{\nu}\right)^{-0.4} + 35,000$

Species properties		Bromine	Bromide	Sulphur	Sulphide
Stoichiometric coefficient	z_P	1	2	1	1
Concentration at σ_{BOC}	$[P]_{BOC}\,(M)$	0.225	4.05	3.575	1.225
Diffusion coefficient	$D\,(\times 10^{10}\,m^2\,s^{-1})$	20	12	5	6
Schmidt number	Sc	385	640	2360	1970

Electrolyte properties		Bromide	Sulphide	Membrane
Electrode membrane gap	$g\,(mm)$	0.95	0.95	0.2
Conductivity	$\kappa\,(S\,m^{-1})$	23	29	1
Kinematic viscosity	$\nu\,(\times 10^6\,m^2\,s^{-1})$	0.77	1.18	–
Electrolyte density	$\rho\,(g\,l^{-1})$	1300	1300	–

umes of each electrolyte were used, although in practice a smaller volume could be considered for the sulphide system due to its high solubility [26].

The change in electrolyte volume $\Delta V\,(m^3)$ occurring after charging for time Δt at constant current density i was found from a mass balance:

$$\Delta V = \frac{t_{H_2O} M_{H_2O} N A i}{\rho_{H_2O} F}\ \Delta t \tag{4}$$

where t_{H_2O} is the transference coefficient for water, M_{H_2O} and ρ_{H_2O} are the molecular weight and density of water, and N is the number of electrochemical cells. The transference coefficient of water t_{H_2O} in Nafion 117 membranes at 25 °C where sodium ions are the charge-carrier is 10 molecules of water per sodium ion transferred [24].

The species concentrations were found from the state-of-charge, the corresponding bromide and sulphide volume V_{Br} and V_S found using Eq. (4), V_{BOC}, and $[Br]_{T,BOC}$ and $[S]_{T,BOC}$ (the total elemental concentrations of bromide and sulphide at bottom-of-charge) as follows:

$$[Br_2]_{V_{Br}} = \frac{1}{2}\frac{V_{BOC}}{V_{Br}}\sigma_{Br}[Br]_{T,BOC} \tag{5}$$

$$[Br^-]_{V_{Br}} = \frac{V_{BOC}}{V_{Br}}(1-\sigma_{Br})[Br]_{T,BOC} \tag{6}$$

$$[S]_{V_S} = \frac{4}{5}\frac{V_{BOC}}{V_S}(1-\sigma_S)[S]_{T,BOC} \tag{7}$$

$$[S^{2-}]_{V_S} = \frac{1}{5}\frac{V_{BOC}}{V_S}(1+4\sigma_S)[S]_{T,BOC} \tag{8}$$

2.2. Energy storage plant specifications

The energy storage plant specification was based on the first utility-scale PSB storage plant constructed by Regenesys Ltd. [1] (although for commercial reasons the plant was never commissioned). The plant was constructed using XL200 modules, which consisted of 200 XL cells assembled to form a bipolar stack. These modules were rated at 120 kW assuming a current of 400 A and a cell voltage of 1.5 V. The plant was specified to give a power output of 15 MW and an energy storage capacity of 120 MWh (corresponding to an 8 h discharge). NaBr and $Na_2S_{4.8}$ electrolytes were used in the sulphide and bromide tanks respectively, with $[Br]_{T,BOC} = 4.5$ M and $[S]_{T,BOC} = 4.8$ M. The electrolyte volume was adjusted in order to deliver 120 MWh of capacity. With these electrolyte compositions:

$$\sigma_S = \frac{75}{128}\sigma_{Br} + \frac{1}{96} \tag{9}$$

In terms of lifetime, the limiting component was expected to be the membrane, which typically lasts 15 years in the harsher chlor-alkali industry [1]. The plant life was therefore assumed to be 15 years, with around 250 cycles of utilisation per year. While the model was capable of modelling self-discharge over a long series of cycles [19,25], the effect of self-discharge was not included in this study. In practice electrolyte conditioning would be required to keep the system in balance. It was therefore assumed that conditioning was carried out regularly, so that the same performance could be expected on each cycle.

2.3. Energy storage plant variables

A key variable was the applied current density, which leads to a trade off between overpotential losses (affecting operating cost) and the number of modules required (affecting capital cost). The

current density was thus optimised in order to minimise the total cost. The current density used during charge and discharge was assumed to be equal.

The electrochemical rate constants were varied in order to determine its effect on process performance and economics. Initially rate constants of 40×10^{-8} and 3×10^{-8} m s^{-1} were used for the bromine and sulphide half-couples respectively (based on data reported in part 1 [19]). The rate constants were then increased to determine whether the use of electrocatalyst could deliver improved technical and economic performance.

When the rate constant was changed, the current density was optimised in each case. Other plant parameters were also altered in order to ensure that the plant met the specification (Section 2.2), including the electrolyte velocity. The velocity was assumed to be constant and equal on both sides of the membrane. In practice, identical pumps are likely to be used and the different properties of the electrolytes and variations in geometries would lead to different velocities, although the differences are likely to be relatively small. The velocity was increased with current density in order to avoid approaching mass-transport limits, and was adjusted to achieve a maximum dimensionless current (the ratio of the applied current density to the limiting current density [19]) of 0.9. This condition invariably occurred for the bromide system at the end of discharge due to the low bromine concentration.

In each case, the number of cells N required to deliver 120 MWh (corresponding to a total energy delivered Q_T of 432 GJ) over an 8 h discharge was found. Assuming that all cells gave the same performance, the number of cells required could be calculated from the energy delivered by a single cell, Q_{del}. Accounting for the pump work required during discharge ($Q_{p,dis}$) and assuming 5% transmission losses [27], Q_{del} is given by

$$Q_{del} = 0.95 \left(iAN \int E_{dis}\ \mathrm{d}t - Q_{p,dis} \right) \tag{10}$$

The integral was calculated by numerically integrating the cell discharge curve obtained from the numerical model [19,25]. $Q_{p,dis}$ was found from the pressure drops and the length of the discharge period t_{dis} (including a 10-min warm-up period):

$$Q_{p,dis} = \frac{t_{dis} A_c \nu (\Delta p_{Br} + \Delta p_S)}{\pi_p} \tag{11}$$

The pressure drops Δp_{Br} and Δp_S (Pa) were found from the relationships given in Table 1 and a pump efficiency π_p of 35% was assumed. The number of cells N was thus obtained from

$$N = \frac{Q_T}{0.95 \left[iA \int E_{dis}\, \mathrm{d}t - ((A_{Chan} \nu T_{dis})/\pi_{pump})(\Delta p_{Br} + \Delta p_S) \right]} \tag{12}$$

N was rounded up to give an integer number of XL200 modules (thus the energy delivered was close to, but not exactly, 120 MWh). The system performance, including the pump work and transmission losses was assumed to be independent of the number of cells used.

In order to determine the required electrolyte volume (V_{BOC}), it was necessary to consider the range of the state-of-charge. It is not normal practice to fully charge or fully discharge the electrolytes as losses increase close to mass-transport limiting conditions. In addition, charged species (particularly bromine) are corrosive and unstable. At high state-of-charge, the volume of the bromine electrolyte decreases and the high concentration of bromine leads to a risk of release of hazardous bromine gas. Hence, the system typically operates with a bromine state-of-charge σ_{Br} between 0.1 and 0.5 [25]. Thus the volume of electrolyte used depends on the change in the state of charge $\Delta\sigma_{Br}$ as follows:

$$V_{BOC} = \frac{z_{Br_2}}{z} \frac{2iANt_{ch}}{[Br]_{BOC}\ \Delta\sigma_{Br} F} \tag{13}$$

where $z/z_{Br_2} = 2$, t_{ch} is the length of the charging cycle and $[Br]_{BOC}$ is the total concentration of bromine atoms (in bromide and bromine) at the bottom-of-charge (i.e. $\sigma_{Br} = 0.1$). In this study values of $t_{ch} = 8$ h, $\Delta\sigma_{Br} = 0.398$ and $[Br]_{BOC} = 4.5$ M were assumed. On this basis the range of state-of-charge for the sulphide electrolyte can be calculated to be $\Delta\sigma_S = 0.233$ [25]. This suggests that there may be scope for using a smaller sulphide electrolyte volume or lower concentrations in order to reduce electrolyte costs. At bottom-of-charge, $\sigma_{S,BOC}$ was 0.069, giving a top-of-charge $\sigma_{S,TOC}$ of 0.302.

3. Commercial model

A commercial model of a redox flow battery plant was developed in order to predict the commercial performance as a function of the technical performance predicted by the model. The goal of this commercial modelling was to evaluate the sensitivity of the plant economics to operating and system parameters such as current density and electrochemical rate constants. While the overall economic outcome is of interest, the commercial parameters are subject to significant variation due to market conditions and local factors.

3.1. Capital costs

Obtaining accurate data on the capital cost of process equipment, particularly for a technology which has not been established is extremely challenging. For this study, an approximate capital cost has been estimated based on a 'best-case' scenario for the commercial performance, assuming a mature RFB industry has been established. The capital cost model was based on an existing model of a PSB system that predicted a capital cost of £320 kW^{-1} [25]. This model assumed 1995 UK prices, a production rate of 400 MW per year of 200 kW-rated modules, mature production costs (representing the middle of the growth phase of the product life cycle), and modularisation and standardisation of plant designs. It was assumed that increased costs due to inflation since 1995 would be offset by savings associated with technological improvements. The capital cost is divided into three elements: electrochemical cells (including balance of plant), electrical equipment and electrolyte and tanks [25].

3.1.1. Electrochemical cell costs: £41,000 for a 120 kW module

The cost of the electrochemical cells includes the material cost (electrodes, membrane, turbulator, endplates, seals, connectors etc.), manufacturing costs (extrusion, welding, assembly, labour etc.), annual production costs (salaries, rent, services, maintenance and depreciation), but not the capital cost of the manufacturing plant. A scaling factor of 2.6 was been recommended for large-scale electrochemical plant [27] to account for the installation costs (piping, instrumentation, safety, labour and taxation). Piping, instrumentation and labour costs were included in the balance of plant cost, so a smaller scaling factor of 1.5 was used for the remaining installation costs, giving an installed module cost of £37,500.

The balance of plant (pumps, heat exchangers, pipework, buildings, and instrumentation) has been estimated to cost £30 kW^{-1}, or £3600 for a 120 kW module [25]. Thus the module and balance of plant costs per module was estimated to be £41,000 per XL200 module. For a plant using a large number of cells, it has been proposed that economies of scale would reduce the balance of plant and installation cost per cell [27]. A power-law relationship between the installed cost and the number of cells was suggested, with an exponent of 0.9. The total cost of the modules C_m was therefore calculated from the number of modules N_m:

$$C_m = \alpha N_m^{0.9} \tag{14}$$

Assuming that for $N_m = 1$, $C_m = £41{,}000$, the constant α can be taken to be £41,000.

3.1.2. Electrical plant: £60 kW^{-1}

The electrical plant including AC–DC power converters, transformers, protection and control systems were assumed to be £60 kW^{-1}. The power requirement was taken as the power consumed on charge P_{mx} (kW) as this was the highest demand the plant encountered.

3.1.3. Electrolyte and tank costs: £350 m^{-3}

The cost of the electrolytes was estimated at £1.0 and £0.23 kg^{-1} for solid NaBr and Na_2S_4 respectively [28]. These estimates used market prices for high-volume orders and assumed the availability of appropriately pure water on site. The polysulphide electrolyte used in this study had the formula $Na_2S_{4.8}$, so the polysulphide cost was increased slightly to £0.25 kg^{-1} to allow for the additional zero-valent sulphur present. The relative molecular masses of NaBr and $Na_2S_{4.8}$ are 103 and 199.6 g mol^{-1} respectively, and with bromide and polysulphide concentrations of 4.5 and 1.0 M, the electrolyte costs were estimated as £460 and £50 m^{-3} respectively. As the electrolyte volumes V_{BOC} were identical, an average electrolyte cost of £250 m^{-3} was used. The costs of electrolyte processing to remove by-products and topping-up with fresh electrolyte were not included.

The electrolyte storage tank costs included installation, a PVDF lining for the corrosive bromine electrolyte and a polypropylene lining for the sulphide electrolyte. The tanks had to be large enough to cope with the variation in electrolyte volume during charging. Allowing for a 40% margin a total tank cost of £100 m^{-3} was estimated [28]. The electrolyte and tank half-couple volumetric costs were combined into a total electrolyte cost of £350 m^{-3}.

Hence, the total capital cost used in this model was found as the sum of three components:

$$C_{cap} = £41,000 N_m^{0.9} + £60 P_{mx} + £350(2V_{BOC}) \quad (15)$$

These capital costs were represented in p kWh^{-1} on the basis that the plant delivered 120 MWh 250 times a year over the plant lifetime of 15 years.

3.2. Operating costs

The critical operating cost was the cost of electrical energy consumed in each cycle. Other costs (e.g. maintenance etc.) were assumed to negligible and insensitive to the plant design. The electrical energy consumed on each cycle included the delivered energy, the losses associated with the inefficiency of the charge and discharge processes (overpotentials and ohmic losses), transmission losses and pump work. The delivered energy was fixed from the design specification at 120 MWh. The energy losses in the charge and discharge process was calculated from numerical integration of the cell voltage profiles from the numerical model:

$$\text{charge energy} - \text{discharge energy} = iAN\left[\int E_{ch}\, dt_{ch} - \int E_{dis}\, dt_{dis}\right] \quad (16)$$

Pumping losses were calculated using Eq. (11), transmission loss was estimated to be 5% of the total delivered energy [i.e. $0.05NQ_{del}$, where Q_{del} is obtained from Eq. (10)] and it was assumed that there were no transmission losses on charge.

The cost of these losses was found using electricity prices. These fluctuate daily and seasonally, and bidding under the New Electricity Trading Arrangement (NETA) can significantly affect prices. Buy and sell prices were estimated from the daily variations in the UK electricity market recorded on the third Wednesday (a typical weekday) of the first month of each quarter in 2006 [29] as shown in Fig. 1. The buy price was always greater than the sell price and each day had at least one peak in buy price, but the time of the peak varied widely. Sell prices were invariably low overnight between 10 *p.m.* and 6 *a.m.* Some seasonal variation was apparent with higher prices in January and April than in July and October.

It was assumed here that the RFB plant was charged between 10 *p.m.* and 6 *a.m.* with energy sourced from a neighbouring power plant at the sell price. The average sell prices for the data in Fig. 1 at this time was £23 MWh^{-1} (2.3 p kWh^{-1}) as shown in Table 2. It was assumed that the operator sold the stored energy (120 MWh) to the customer during the 8 daytime hours (6 *a.m.*–10 *p.m.*) at the maximum buy price. The times at which the electricity was sold for

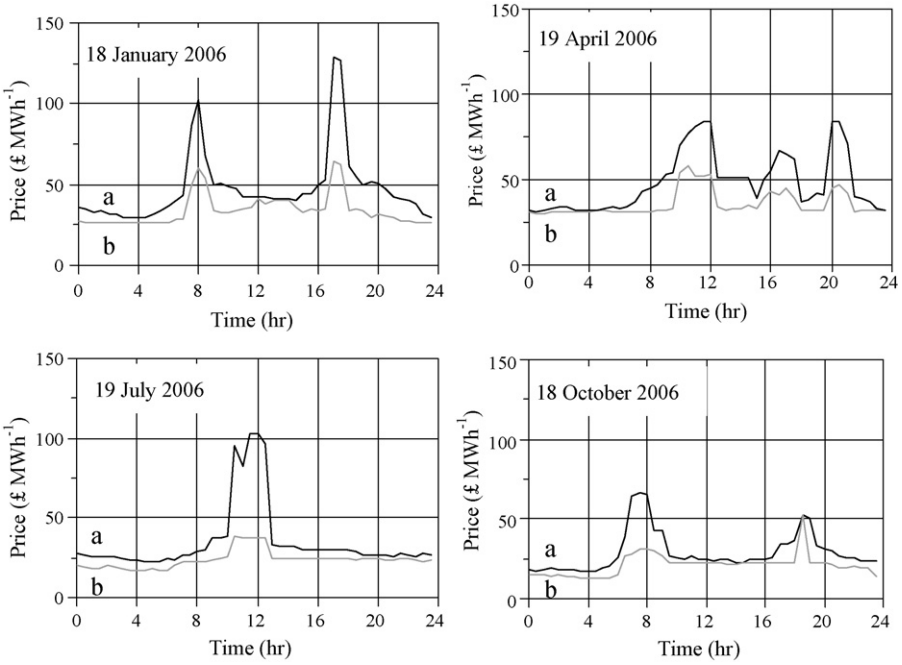

Fig. 1. Recorded UK grid electricity buy and sell prices for the third Wednesday of the first month in each quarter of 2006 [28]: (a) buy price; (b) sell price.

Table 2
Average electricity buy and sell prices for the data in Fig. 1 and the time periods at which the electricity was bought and sold.

	Average sell price (£ MWh^{-1})	When stored	Average buy price (£ MWh^{-1})	When delivered
18 January 2006	26.6	10 *p.m.*–6 *a.m.*	67.1	7–10 *a.m.*, 4–9 *p.m.*
19 April 2006	31.1	10 *p.m.*–6 *a.m.*	67.7	9 *a.m.*–1 *p.m.*, 4–6 *p.m.*, 8–10 *p.m.*
19 July 2006	19.8	10 *p.m.*–6 *a.m.*	52.6	9 *a.m.*–5 *p.m.*
18 October 2006	15.0	10 *p.m.*–6 *a.m.*	42.2	6–10 *a.m.*, 5–9 *p.m.*
Average	23.1		57.4	

the data in Fig. 1 is shown in Table 2; the average best buy price available was found to be £57 MWh^{-1} (5.7 p kWh^{-1}). The buy and sell prices fluctuate considerably and the prices used in this study are guide values only. The cost of the energy used was calculated at a sell price of 2.3 p kWh^{-1}. This cost per cycle was multiplied by 250 cycles to give the annual cost. The lifetime cost was found using a net present value (NPV) factor ω [24]:

$$\omega = \frac{1 - ((1+a)/(1+r))^n}{\ln((1+r)/(1+a))} \quad (17)$$

An annual inflation rate a and discount rate r of 2.5% and 10% were used respectively [1]. For a plant lifetime of 15 years $\omega = 9.25$, and the plant annual cost was multiplied by ω to predict the lifetime operating cost. This cost was divided by the total energy delivered (i.e. 120 MWh cycle^{-1} with 250 cycles per year over 15 years) to give a cost in p kWh^{-1} delivered.

3.3. Total cost and net profit

The total cost in p kWh^{-1} of the plant was offset by the income generated by selling the stored electrical energy at a peak rate of 5.7 p kWh^{-1}. The total revenue was multiplied by the net present value factor ω. The cost model used is summarised in Table 3. The cost model used was systematic, wide-ranging in scope and based on figures expected for mature, high-volume technology and industry best practice. However, its accuracy was limited by the assumptions used, the simple scale factors and the variability of the pricing data. The resulting commercial predictions should be taken as indicative only.

4. Results and discussion

4.1. Optimisation of current density

The predicted effect of current density on the number of XL200 modules and half-couple electrolyte volume V_{BOC} required (for the technical and commercial parameters given in Tables 1 and 3) is shown in Fig. 2. As expected, the number of modules required fell as the current density increased. A least-squares fit to a power-law relationship over the range of current density investigated showed that the variation of the number of modules with current density had an exponent of −0.80, i.e. the variation can be expressed as

$$N = \alpha i^{-0.80} \quad (18)$$

The relationship was not exactly inversely proportional as cell losses increased with current density. This relationship ceased to hold at high currents when the velocity increased and pump work became significant. The electrolyte volume required increased gradually with current density, increasing by 40% over the range investigated. The power-law exponent for the electrolyte volume with current density was 0.20, as expected [Eqs. (13) and (18)].

The variation in the electrolyte velocity required is shown in Fig. 3. The exponent for the power-law variation of velocity with current density was 1.11 for the range investigated. The strong

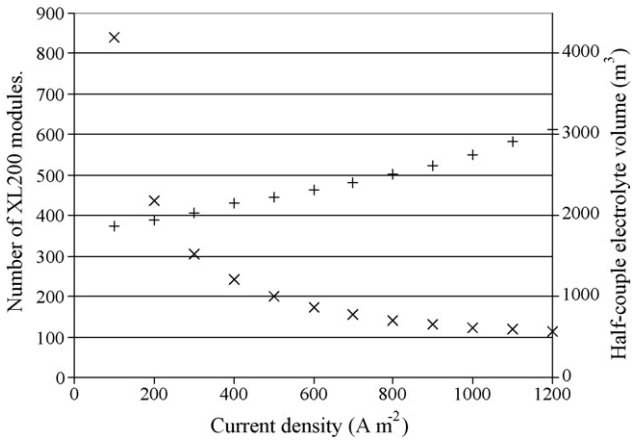

Fig. 2. Effect of current density on the number of modules (N) and electrolyte volume (V_{BOC}) required to deliver 120 MWh: (×) N; (+) V_{BOC} (m^3).

Table 3
Commercial model parameters.

Overall design	Required delivered energy	120 MWh per cycle at 15 MW
	Charge/discharge period	8 h
	Frequency of charge cycles	250 cycles year^{-1}
	Plant lifetime	15 years
Capital cost	Installed module/BOP capital cost	£41, 000$N_m^{0.9}$
	Electrical plant cost	£60 kW^{-1} on charge
	Electrolyte/tank cost	£350 m^{-3}
Running costs and income	Pump efficiency, π_p	35%
	Transmission losses	5% on discharge
	Cost of electricity consumed	2.3 p kWhr^{-1}
	Value of electricity delivered	5.7 p kWhr^{-1}
Net present value calculation	Inflation rate, a	2.5%
	Discount rate, r	10%
	Net present value factor, ω	9.25 years

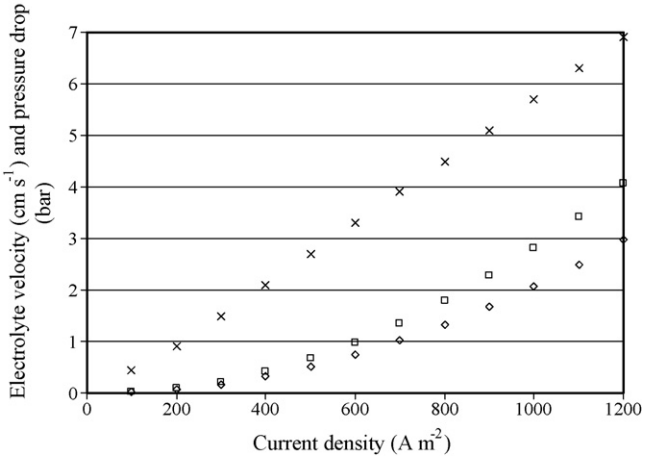

Fig. 3. Effect of current density on calculated electrolyte velocity and pressure drops: (×) v (cm s^{-1}); (□) Δp_{Br} (bar); (◊) Δp_S (bar).

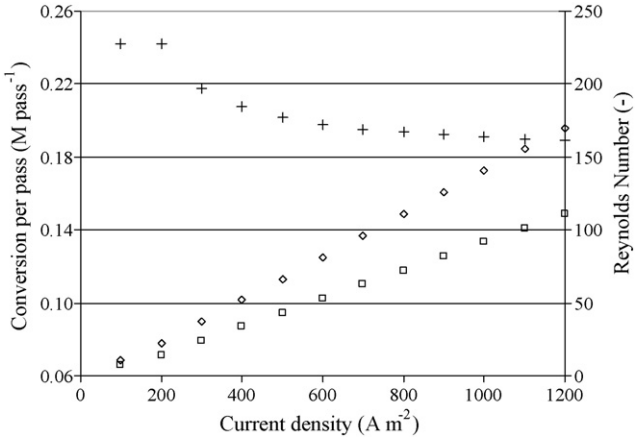

Fig. 4. Effect of current density on the calculated Reynolds number and extent of reaction per pass and: (+) ψ_{Br^-} (M pass^{-1}); (◊) Re_{Br}; (□) Re_S.

dependence of the pressure drop Δp on velocity led to a rapid increase in pressure drop with current density, with a power-law exponent of 2.1. The pressure drop in the bromide electrolyte was greater than that in the sulphide electrolyte despite the lower viscosity. This difference is due to the different pressure drop relationships shown in Table 1.

The extent of reaction per pass ψ was found to decrease slightly with current density. This follows from Eq. (3), since ψ is determined from both i and v. As shown in Fig. 4, ψ remained below 0.39 M pass^{-1} for bromide ions. Note that the extent of reaction for bromine, sulphur and sulphide will be exactly half that of bromide due to the stoichiometry and the assumption that the current efficiency was 100%. The variation of Reynolds number with current density is also shown in Fig. 4. In most cases the Reynolds number was within the range specified for the mass-transport correlations given in Table 1. However, at the highest and lowest current densities there is some uncertainty in the mass transfer coefficients used.

The variation in overall energy efficiency π, energy density and power density with current density is shown in Fig. 5. The energy efficiency decreased from 83% to 39% over the range of current density investigated due to rising cell electrical losses and pumping requirements. A least-squares fit to a power-law relationship gave the exponent for the variation of efficiency with current density as −0.30. The energy density, defined as the energy delivered on discharge (i.e. 120 MWh) per unit volume of electrolyte, also decreased as the current density increased. The power density, defined as the

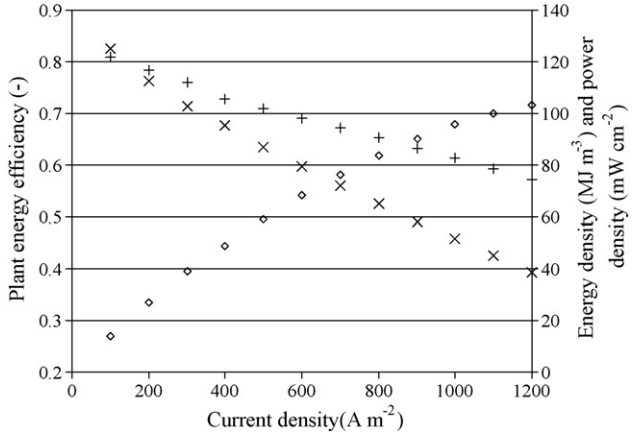

Fig. 5. Effect of current density on energy efficiency, power an energy density: (×) π; (◊) power density (mW cm^{-2}); (+) energy density (MJ m^{-3}).

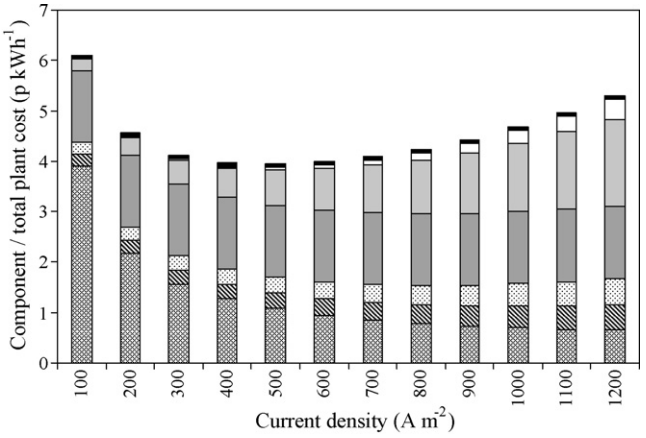

Fig. 6. Effect of current density on plant component and net cost (p kW^{-1}): (▨) module/BOP cost; (▧) electrical plant cost; (⬚) electrolyte/tank cost; (▩) delivered electricity cost; (▩) cell inefficiency cost; (□) pumpwork cost; (■) transmission loss cost.

discharge power (i.e. 15 MW) per unit area, increased as the current density increased as expected.

The predicted contribution of the various cost components to the total cost, and their variation with current density, is shown in Fig. 6. The capital costs of the modules and balance of plant dominated at low currents, but quickly tailed off. The inefficiency cost rose throughout due to increasing overpotential and resistive losses, and dominated at high current density. The electrical plant cost and electrolyte/tank cost both rose steadily. The pumping cost was small initially, but rose rapidly such that it became the highest cost component at high current density. The transmission cost was constant, and was a small fraction of the total cost.

Fig. 6 shows that a minimum in the total cost of the stored electrical energy of 3.97 p kWh^{-1} was obtained at an optimum current density of 500 A m^{-2}. The overall efficiency at this current density was found to be 64%. This optimum was relatively shallow such that a range of current densities (300–700 A m^{-2}) led to a similar cost. The net profit of the plant was found by subtracting this net cost from the income derived by selling the 120 MWh of electricity delivered at 5.7 p kWh^{-1}, summed over the lifetime of the plant using the NPV factor. The net 'profit' is shown in Fig. 7, although this was negative (indicating a loss) throughout the range of current density investigated, with a minimum loss of 0.45 p kWh^{-1} at a current density of 500 A m^{-2}. This equated to a net loss of £1.3 million over the plant lifetime. This suggests that the proposed 15 MW/120 MWh PSB plant would not be profitable if used solely for arbitrage.

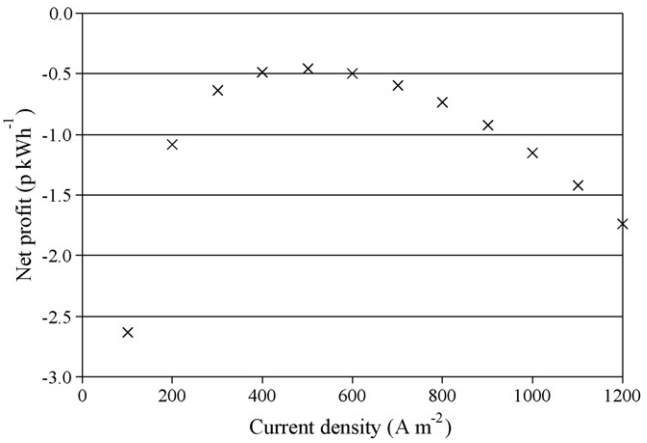

Fig. 7. Effect of current density on net profit.

4.2. Effect of reaction kinetics

One method for improving the plant commercial performance would be to improve the reaction kinetics. This would reduce the overpotential losses, but could increase costs elsewhere e.g. the module cost could rise if an expensive electrocatalyst were used. However, in the Regenesys PSB system no catalyst was used and it is possible that a relatively cheap catalyst such as nickel could substantially improve the kinetics of the bromide–polysulphide couple without significantly increasing the electrode cost [7]. The effect of improving the rate constant was investigated assuming there was no impact on the commercial parameters.

The kinetic rate constants used above were 4×10^{-7} and 0.3×10^{-7} m s^{-1} for the bromide and sulphide systems respectively. The effect increased rate constants of 5×10^{-7}, 10×10^{-7} and 100×10^{-7} m s^{-1} for both half-couples was investigated. In each case the current density was varied as before to determine the performance at optimum conditions. It has been reported elsewhere [25] that changing the rate constants had no effect on electrolyte velocity. Increasing the rate constant slightly reduced the required number of modules, the electrolyte volume and the energy stored while slightly increasing the average cell voltage during discharge, the energy efficiency, the power density and the energy density due to the smaller overpotential losses. Commercially, the cost of the modules and BOP and the cost of the pump work decreased due to the smaller number of modules, the cell inefficiency cost fell due to the decrease in overpotential losses, the electrolyte tank cost fell due to the decrease in the electrolyte volume, and the electrical plant cost fell due to the reduced power rating on charge. These cost reductions were all relatively small, but combined to have a significant cost reduction overall, as shown in Fig. 8. It was found that increasing both rate constants from 4×10^{-7} and 0.3×10^{-7} m s^{-1} for the bromide and sulphide systems respectively to 100×10^{-7} m s^{-1} for both half-couples increased the net profit at the optimum current density from −0.45 to +0.15 p kWh^{-1}. Thus a relatively small improvement in rate constant was sufficient to make the system economic for arbitrage. The improvement in profit was largest at high current, where the reduction in losses had the most effect. The optimum current density increased slightly, to around 600 A m^{-2}.

4.3. Sensitivity to economic parameters

There is significant uncertainty in the capital costs used in this study. Capital costs could be reduced by technological breakthroughs, improved manufacturing procedures and economies of scale. It was found that, if costs were reduced by around 25% (capital costs of electrochemical cells reduced from £41,000 to £30,000 per 120 kW module, electrolyte/tank cost reduced from £350 to £250 m^{-3} and electrical plant cost reduced from £60 to £45 kW^{-1}) then the plant became economic for arbitrage (see Fig. 9). A slight profit of +0.03 p kWh^{-1} was obtained at an optimum current density of 400 A m^{-2}.

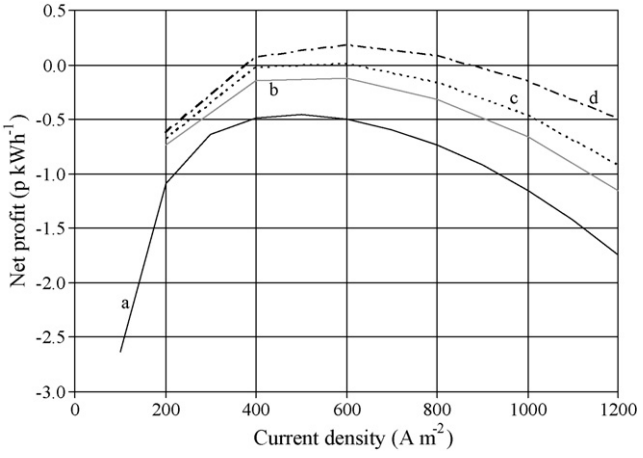

Fig. 8. Effect of rate constant and current density on net profit: (a) $k_{s,Br} = 4 \times 10^{-7}$ and $k_{s,S} = 0.3 \times 10^{-7}$ m s^{-1}; (b) $k_{s,Br} = k_{s,S} = 5 \times 10^{-7}$ m s^{-1}; (c) $k_{s,Br} = k_{s,S} = 10 \times 10^{-7}$ m s^{-1}; (d) $k_{s,Br} = k_{s,S} = 100 \times 10^{-7}$ m s^{-1}.

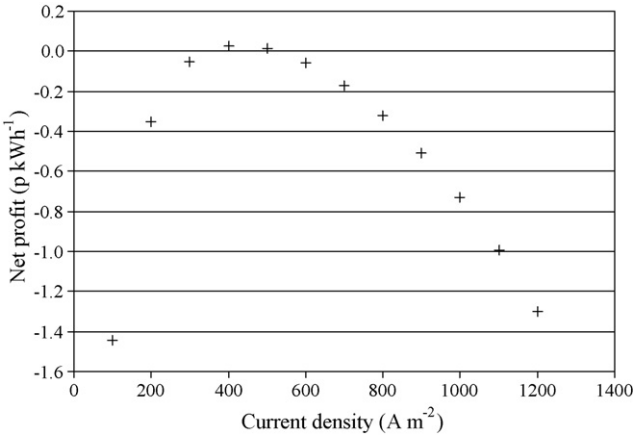

Fig. 9. Effect of current density on net profit for a 20–30% reduction in cost parameters (module/BOP capital cost reduced from £41,000 to £30,000, electrolyte/tank cost reduced from £300 to £250 m^{-3}, and electrical plant cost reduced from £60 to £45 kW^{-1}).

Similarly, it was found that the commercial performance was sensitive to the price of electricity, and that a slight improvement in the sell and buy price electricity from 2.3 and 5.7 p kWh^{-1} to 2.0 and 6.0 p kWh^{-1} respectively was sufficient to make the plant profitable with a net profit of +0.02 p kWh^{-1} at a current density of 500 A m^{-2}. The sell price can be reduced by negotiating a favourable contract with a nearby generator, and the buy price may rise in the near future in the UK due to fuel shortages. The increased use of renewable energy sources such as wind power is also likely to increase the buy price during periods of peak demand and such improvements are certainly feasible.

5. Conclusions

This study illustrates how technical parameters can be linked to commercial performance for an electrochemical energy storage system. The technical model can be used to identify the parameters which limit performance and to identify how this performance limitation is related to the commercial viability of the process. In addition, with accurate commercial data the model can be used to provide targets for technical improvements such as electrochemical rate constants in order to develop a viable technology. The technical model could be improved by accounting for factors such as shunt currents in the bipolar stacks and the occurrence of side reactions as mass transport limiting conditions are approached. Although the commercial model used a fairly simplistic approach, the link between technical and commercial performance (for example optimisation of current density) was readily achievable.

Increasing the current density was found to decrease the required number of modules to deliver the design specification, increase the electrolyte volume, increase the electrolyte velocity, and decrease the cell efficiency. Based on the technical and commercial parameters used, the system was found to be uneconomic for the range of current densities investigated, with a maximum net profit of −0.45 p kWh^{-1} at an optimum current density of 500 A m^{-2}. It was found that an increase in the electrochemical rate constants from 4×10^{-7} and 0.3×10^{-7} m s^{-1} to 10^{-5} m s^{-1} (for

both electrolytes), without incurring a cost penalty, was sufficient to make the plant economic for arbitrage applications. Additionally, the plant could be made economic by reducing capital costs by 20–30% or an improved buy and sell price differential for electrical energy. Although these results suggest that RFB systems may not be economic in the current climate, it seems likely that such systems will become increasingly profitable as investment in renewable electricity generation accelerates.

Acknowledgements

The authors are grateful to the Engineering and Physical Sciences Research Council (UK) and to Regenesys Technologies (UK) Ltd. for the funding provided for this research.

References

[1] EPRI-DOE Handbook of Energy Storage for Transmission and Distribution. EPRI and the US Department of Energy, 1001834 (2003).
[2] Regenesys utility scale energy storage: project summary. DTI reports available online at: http://www.ecdti.co.uk/cgibin/perlcon.pl (Accessed 01 August 2006).
[3] M. Bartolozzi, J. Power Sources 27 (1989) 219–234.
[4] C. Ponce de Leon, A. Frias-Ferrer, J. Gonzalez-Garcia, D. Szanto, F. Walsh, J. Power Sources 160 (2006) 716–732.
[5] VRB Power Acquires Regenesys Electricity Storage Technology. 5th October 2004. URL: http://powerelectronics.com/news/vrb-power-regenesys (Accessed October 2008).
[6] A. Price, S. Bartley, S. Male, G. Cooley, Power Eng. J. 13 (1999) 122–129.
[7] P. Zhao, H. Zhang, H. Zhou, B. Yi, Electrochim. Acta 51 (2005) 1091–1098.
[8] H. Zhou, H. Zhang, P. Zhao, B. Yi, Electrochim. Acta 51 (2006) 6304–6312.
[9] E. Sum, M. Skyllas-Kazacos, J. Power Sources 15 (1985) 179–190.
[10] M. Skyllas-Kazacos, V. Geol, Proc. Appl. Com. 2002 (2002) 63–78.
[11] M. Skyllas-Kazacos, J. Power Sources 124 (2003) 299–302.
[12] High capacity electrical storage. URL: http://pluronsystems.com (Accessed October 2008).
[13] B. Fang, S. Iwasa, Y. Wei, T. Arai, M. Kumagai, Electrochim. Acta 47 (2002) 3971–3976.
[14] A. Paulenova, S. Creager, J. Navratil, Y. Wei, J. Power Sources 109 (2002) 431–438.
[15] P. Fedkiw, R. Watts, J. Electrochem. Soc. 131 (1984) 701–709.
[16] N. Koshel, V. Zvychainyi, Russ. J. Electrochem. 33 (1997) 904–909.
[17] R. White, S. Lorimer, J. Electrochem. Soc. 130 (1983) 1096–1103.
[18] T. Evans, R. White, J. Electrochem. Soc. 134 (1987) 2725–2733.
[19] D.P. Scamman, G.W. Reade, E.P.L. Roberts, J. Power Sources 189 (2009) 1220–1230.
[20] M. Gattrell, J. Park, B. MacDougall, S. McCarthy, J. MacDonald, V. Geol, Proc. Appl. Com. (2002) 79–94.
[21] M. Chakrabarti, R. Dryfe, E. Roberts, Electrochim. Acta 52 (2007) 2189–2195.
[22] C. Ponce-de-Leon, G. Reade, I. Whyte, S. Male, F. Walsh, Electrochim. Acta 52 (2007) 5815–5823.
[23] T. Okada, S. Moller-Holst, O. Gorseth, S. Kjelstrup, J. Electroanal. Chem. 442 (1998) 137–145.
[24] D. Scamman, EngD Thesis, University of Manchester, Manchester, 2007.
[25] F. Walsh, A First Course in Electrochemical Engineering, The Electrochemical Consultancy, Romsey, Hants, England, 1993.
[26] S. Licht, J. Electrochem. Soc. 134 (1987) 2137–2141.
[27] F. Goodridge, K. Scott, Electrochemical Process Engineering: A Guide to the Design of Electrolytic Plant, Plenum Press, New York, 1995.
[28] T. Calver, D. Clark, G. Cooley, W. Cranstone, A. Elliott, A. Hebbs, S. Male, P. Mitchell, M. Patrick, J. Newton, S. Oates, J. Robertson, I. Whyte, Regenerative fuel cell technical report. National Power Ltd. (UK) Report Number TECH/JFB 8600/038, 1997.
[29] UK electricity balancing and settlement reports: pricing data. Elexon Ltd. (UK). URL: http://www.elexon.co.uk/marketdata/PricingData/default.aspx (Accessed December 2006).